

# Unoccupied dimer-bond state at Si(001) surfaces

Thomas Fauster

*Lehrstuhl für Festkörperphysik, Universität Erlangen-Nürnberg, D-91058 Erlangen, Germany*

Shin'ichiro Tanaka and Katsumi Tanimura

*The Institute of Scientific and Industrial Research, Osaka University, Osaka, Japan*

(Received 14 November 2011; revised manuscript received 9 December 2011; published 27 December 2011)

Two-photon photoemission is used to identify the unoccupied dimer-bond state on the Si(001) surface at an energy 2.83 eV above the valence-band maximum. A strong resonance enhancement is found for excitation from the occupied dangling-bond state. The azimuthal and polarization dependence proves the orientation of the observed state along the dimer axis. The dispersion is dominated by the occupied initial state described by  $-0.50$  free-electron masses in one- and two-photon photoemission.

DOI: [10.1103/PhysRevB.84.235444](https://doi.org/10.1103/PhysRevB.84.235444)

PACS number(s): 79.60.Bm, 73.20.At

## I. INTRODUCTION

The covalent bonds of silicon leave a large number of dangling bonds at the surface of a truncated bulk crystal. The associated large energy cost leads to pronounced surface reconstructions to minimize the number of dangling bonds. At the Si(001) surface, the truncated bulk crystal has two dangling bonds per surface atom. This number is reduced to one by dimer formation of neighboring pairs of surface atoms. This is in agreement with the  $(2 \times 1)$  surface reconstruction observed by low-energy electron diffraction. At low temperatures, a  $c(4 \times 2)$  reconstruction forms, which consists of alternately buckled dimers within and perpendicular to the plane shown in Fig. 1. The asymmetric dimerization further reduces the surface energy and leads to an occupied surface state  $D_{\text{up}}$  at the upper dimer atom and an unoccupied counterpart  $D_{\text{down}}$  at the lower dimer atom (see Fig. 1). The two dimer atoms are coupled by a dimer bond and attached to the bulk via back bonds. The dimerization can be observed easily by scanning tunneling microscopy. The asymmetric nature has been elusive due to the rapid flipping of the dimers even at low temperature.<sup>1</sup> Photoemission experiments identified the occupied surface states and found a nonmetallic surface band structure.<sup>2-4</sup> Theoretical calculations unambiguously showed that only asymmetric dimers could explain the semiconducting surface band structure.<sup>5</sup> In addition, the  $c(4 \times 2)$  reconstruction was found to be the structure with the lowest energy.<sup>6,7</sup>

Numerous studies have characterized the surface states of the Si(001) surface in considerable detail.<sup>4,8-11</sup> However, the unoccupied dimer bond (labeled *dimer bond\** in Fig. 1) has not been reported so far. Due to its antibonding nature, it might play an important role in breaking up dimers, e.g., in laser-induced damage or desorption.<sup>12,13</sup> In this work, we use two-photon photoemission to excite the unoccupied dimer bond resonantly from the occupied surface state  $D_{\text{up}}$ . The orientation of the orbital along the dimers is found by polarization-dependent studies on samples with unequal percentages of  $(2 \times 1)$  and  $(1 \times 2)$  areas.

## II. EXPERIMENT

Boron-doped *p*-type Si(001) wafers with resistivity of 4.8 and 5.1  $\Omega\text{cm}$  were clamped with Ta sheets to the

sample holder in an ultrahigh vacuum chamber (base pressure  $<5 \times 10^{-11}$  Torr). Surface structures were characterized *in situ* by a scanning tunneling microscope prior to photoemission measurements. The (001) surfaces were well-ordered double-domain  $(2 \times 1)$  structures with a typical surface-defect concentration of 1%. A Ti-sapphire laser with a repetition rate of 76 MHz was used to generate fs-laser pulses from 700 to 880 nm. The second harmonic of the fundamental generated by frequency doubling in a  $\beta$ -barium-borate crystal (BBO) was used in two-photon photoemission experiments. The temporal width of the pulses was typically 80 fs. Additional one-photon photoemission data were acquired by the fourth harmonic obtained after frequency-doubling the second harmonic. The BBO crystal limited the available photon energy of the fourth harmonic to less than 6.1 eV. Except for the dispersion measurements, data were taken at normal emission for light incident at an angle of  $45^\circ$  relative to the surface normal. *s*- as well as *p*-polarized light could be chosen. Electrons emitted along the surface normal ( $\pm 2^\circ$ ) were analyzed using a hemispherical analyzer with an instrumental energy resolution of 50 meV. The sample temperature was 90 K. Measurements at room temperature gave similar results.

## III. RESULTS

### A. Comparison of one- and two-photon photoemission

Figure 2 shows a series of two-photon photoelectron spectra from Si(001) for photon energies below 3 eV. The data were normalized at the low-energy cutoff. All spectra show a pronounced peak close to the high-energy cutoff. The kinetic energy of the peak varies with twice the photon energy, indicating a transition originating from an initial state. In the corresponding one-photon photoemission spectra taken with frequency-doubled photons, this peak is seen only for  $2 \times 3.00$  eV photon energy with rather low intensity. These observations clearly indicate the participation of an intermediate state in the two-photon photoemission process.

The main peak of the spectra shows a pronounced dispersion with changing parallel momentum. To achieve this, the emission angle was changed in the plane sketched in Fig. 1. Due to the double-domain surfaces the dispersion was measured simultaneously also along the dimer rows

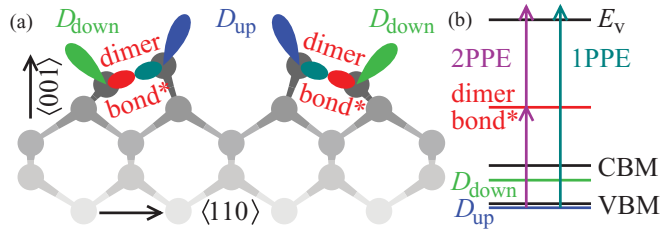


FIG. 1. (Color online) (a) Asymmetric dimer reconstruction of the Si(001) surface showing schematically the dangling-bond orbitals and the antibonding dimer-bond orbital. (b) Two-photon photoemission scheme involving the relevant electronic states.

perpendicular to the plane of drawing. The resulting two-photon photoemission data are shown in Fig. 3 for three different photon energies by filled symbols. For comparison, results obtained by one-photon photoemission with the frequency-doubled photons are shown. All data show a downward dispersion, which can be described by an effective mass of  $0.50 \pm 0.05$  in units of the free-electron mass. This value is larger than the heavy-hole effective mass. Combining this observation with the energy 0.1 eV below the valence-band maximum, the observed peak is assigned to the occupied surface state  $D_{up}$ .<sup>14</sup>

### B. Photon-energy dependence

In order to identify the intermediate state, we extended the two-photon photoemission measurements over a larger range of photon energies in Fig. 4. The spectra were taken with constant pulse energy and width (80 fs). The offset of the spectra is proportional to the photon energy as given on the scale at the right. The intensities measured with  $s$ -polarized light were multiplied by a factor of 5 to give comparable intensities as for  $p$ -polarized light. The main peak at high kinetic energies can be observed at all photon energies, but with reduced intensity between 3.0 and 3.3 eV. Weak peaks can be detected at kinetic energies around 0.5 and 1.0 eV, in particular for high photon energies (see enlarged traces at top of Fig. 4). An additional peak is observed around

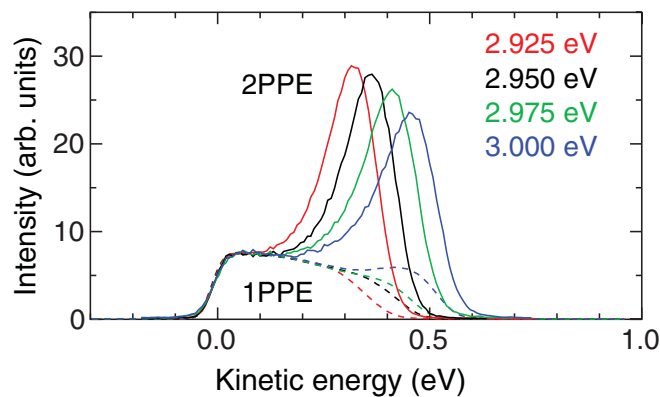


FIG. 2. (Color online) One- and two-photon photoelectron spectra from Si(001) for various photon energies normalized at the low-energy cutoff. One-photon photoemission spectra were taken with twice the photon energy as the corresponding two-photon photoemission spectra.

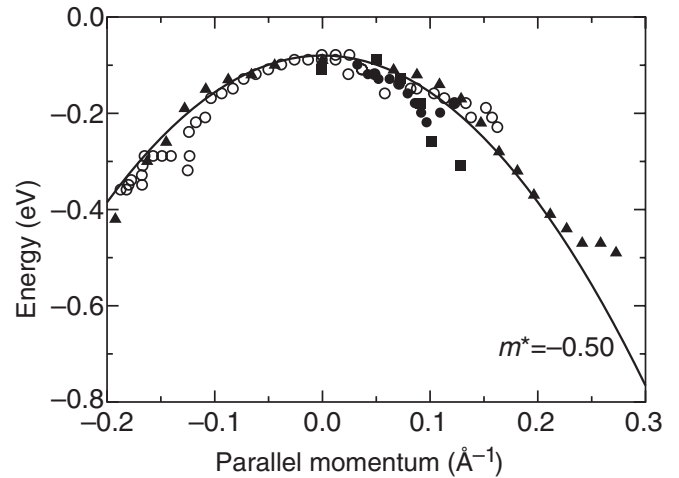


FIG. 3. Dispersion of the main peak obtained by one-photon photoemission with  $h\nu = 6.02$  eV (open circles) and two-photon photoemission with  $h\nu = 2.92$  eV (filled circles), 3.02 eV (filled squares), and 3.45 eV (filled triangles).

0.2 eV for  $p$ -polarization only at the highest photon energies. The structure at 0.5 eV kinetic energy persists for all photon energies, suggesting a final-state feature. The other peaks shift to lower kinetic energy with decreasing photon energy.

The kinetic energies of the peaks are plotted in Fig. 5 as a function of photon energy. The range of photon energies is extended with data from the literature.<sup>14,15</sup> The main peak falls on a straight line with slope  $dE_{kin}/d h\nu = 2$  indicating an initial state at an energy 0.12 eV below the valence-band maximum. For reference to the valence-band maximum, the ionization energy of 5.40 eV has been used.<sup>14</sup> The measured energy confirms the assignment to the occupied surface state  $D_{up}$ .

The peak at 0.9 eV kinetic energy (open triangles in Fig. 5) can be joined by a straight line to the data points for peak B from Shudo and Munakata<sup>15</sup> and the data points for peak E from Kentsch *et al.*<sup>14</sup> The slope of 1 is in agreement with an intermediate state, which is placed at an energy 2.83 eV above the valence-band maximum. For a photon energy of 2.95 eV, the lines for the initial and intermediate states cross and a resonant transition might occur. The spectra in Fig. 4 show indeed a strong intensity enhancement in this photon-energy range. This resonance can be seen more clearly in Fig. 6. The maximum intensity is observed at 2.95 eV photon energy. The width is around 0.20 eV, which is only slightly larger than the spectral width of 0.14 eV of the  $D_{up}$  peak in Fig. 2. The large peak widths are in agreement with the fact that both states are located in the continuum of conduction- and valence-band states, respectively.

The peak observed around 0.2 eV kinetic energy for high photon energies in Fig. 4 is represented by filled squares in Fig. 5. It can be assigned to states near the  $L_1$  point of the band structure (see inset in Fig. 5).<sup>16</sup> For higher photon energies, it matches the low-energy part of the data (peak B) from Shudo and Munakata.<sup>15</sup> The assignment to bulk transitions along the  $\frac{2}{3}\Sigma L$  line followed by an umklapp due to the  $(2 \times 1)$  reconstruction of the Si(001) surface seems to hold as indicated by the lines labeled  $+ \rightarrow +$  and  $- \rightarrow +$  in Fig. 5. The lines

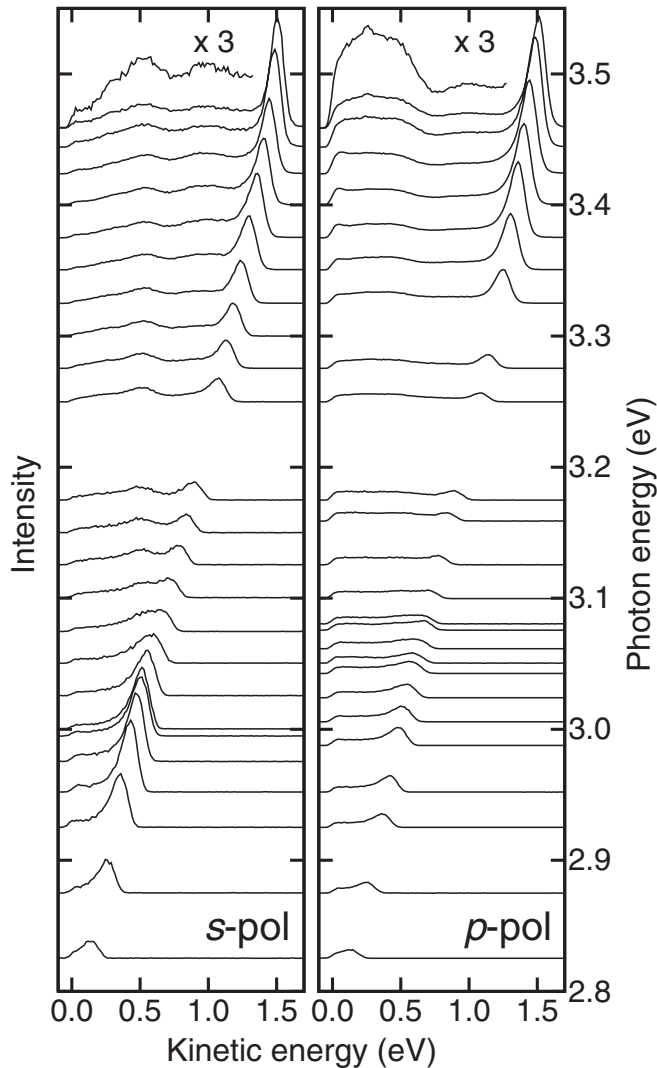


FIG. 4. Two-photon photoelectron spectra from Si(001) for *s*- and *p*-polarized light. The spectra are offset proportional to the photon energy indicated at the right.

for bulk transitions were obtained from the band-structure calculation of Rohlfiing<sup>14</sup> incorporating GW corrections to obtain the correct band gap and quasiparticle energies for electrons and holes.

The structure seen at a constant kinetic energy of 0.5 eV indicates a final state feature around 5.9 eV above the valence-band maximum. The band structure (see inset of Fig. 5) shows only a  $\Delta_5$  band, which does not couple to a free-electron wave function in vacuum. The bands starting at the  $L_3$  point along the  $\frac{2}{3}\Sigma L$  line end around 6 eV. Above this energy, a band gap of 1 eV width opens. These findings point toward a small emission probability from bulk transitions for energies above 6 eV, which might cause a peaklike structure at 0.5 eV kinetic energy.

### C. Dimer-bond orientation

Figure 7 shows the two-photon photoemission intensity for  $h\nu = 2.97$  eV near resonant excitation from the occupied state  $D_{\text{up}}$  to the dimer-bond state as a function of azimuthal

orientation of the sample. The sample was prepared with a 2:1 ratio of the two domains with orthogonal dimer orientation, as sketched in Fig. 7. The ratio was checked by scanning tunneling microscopy. The highest intensity is observed when the polarization vector is aligned along the predominant dimer orientation. This holds for *s*- as well as for *p*-polarized light. The relative intensity between the curves for *s*- as well as for *p*-polarization agrees with the prediction from the optical constants for light incidence at  $45^\circ$ . The azimuthal dependence is well described by the sum of a  $\cos^4$  and a  $\sin^4$  term with the amplitude ratio in agreement with the 2:1 ratio of the two domain orientations (see curves in Fig. 7). The fourth-order dependence proves that a second-order process is observed indeed. In addition, dipole-selection rules confirm that the excitation occurs between two states of even symmetry with respect to the (110) mirror plane. As can be seen from the sketch in Fig. 1, the dangling bonds as well as the dimer bond are derived from orbitals in the mirror plane that have even symmetry under reflection.

## IV. DISCUSSION

In previous work, the intermediate state at 2.83 eV was assigned to a bulk transition between even states along the  $\frac{2}{3}\Sigma L$  line followed by an umklapp due to the  $(2 \times 1)$  reconstruction of the Si(001) surface.<sup>14</sup> This interpretation cannot be correct for photon energies below the optical band gap of Si at 3.4 eV, where the line marked  $+\rightarrow+$  in Fig. 5 ends. The bulk band structure of Si along the (001) direction<sup>14</sup> only shows strongly dispersing bands around 2.8 eV. This holds also for the  $\frac{2}{3}\Sigma L$  line accessible due to the  $(2 \times 1)$  reconstruction and the additional umklapp processes from the  $c(4 \times 2)$  reconstruction. Considering the strong resonance of the intermediate state with the  $D_{\text{up}}$  surface state, we have to look for an unoccupied surface state in this energy range. Most surface band-structure calculations focus on the occupied ( $D_{\text{up}}$ ) and unoccupied ( $D_{\text{down}}$ ) dangling-bond bands.<sup>17</sup> The state under consideration here is degenerate with strongly dispersing bulk bands, which makes it difficult to identify by band-structure calculations employing finite slabs. The semi-infinite bulk can be treated by scattering-theoretical methods.<sup>18</sup> Indeed, Krüger and Pollmann find at the center of the surface Brillouin zone at an energy around 2 eV a dimer-bond state,<sup>18,19</sup> which is derived from the bridge-bond orbitals of the unreconstructed surface.<sup>20</sup> These calculations were performed using the local-density approximation of density-functional theory and underestimate the bulk-band gap by  $\approx 0.5$  eV.<sup>18</sup> A simple correction of the band gap would place the energy of the dimer-bond state around 2.5 eV above the valence-band maximum. A full-fledged calculation of the excited states by a GW scheme<sup>21,22</sup> might add further corrections. Note that the observed peak position at resonance might also be shifted by a Fano-type profile.<sup>23</sup>

After identifying the new state at an energy of 2.83 eV above the valence-band maximum and assigning it to the unoccupied dimer-bond state, the question arises why it has not been seen before. The first inverse-photoemission spectra from Si(001) showed a broad peak at an energy around 2.9 eV above the valence-band maximum, which disappeared upon oxygen adsorption and was not discussed further.<sup>24</sup> A later

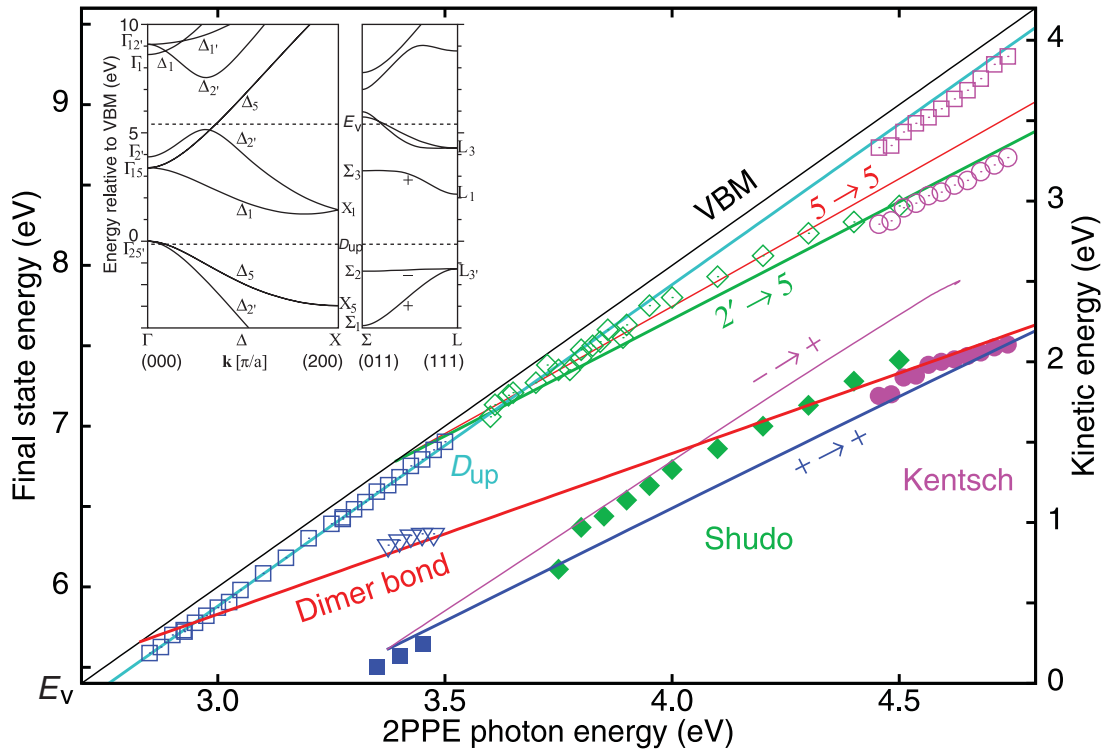


FIG. 5. (Color online) Kinetic energy of the observed peaks as a function of photon energy compared to calculated bulk transitions.<sup>14</sup> The data for photon energies between 3.6 and 4.5 eV are from Ref. 15 and above 4.4 eV from Ref. 14, respectively. The inset shows the relevant ranges of the band structure.<sup>14</sup>

study found an unoccupied state at an energy of 3.05 eV above the valence-band maximum.<sup>11</sup> This state was assigned to the  $\Gamma_{15}$  conduction band, which is known from the optical band gap to lie in energy 3.4 eV above the valence-band maximum. The inverse photoemission data show no significant dispersion with initial-state energy between 14.5 and 18.5 eV, as expected for a surface state. Therefore, it is plausible that the unoccupied state measured at 3.05 eV by inverse photoemission is actually the dimer-bond state. The difference to the value of 2.83 eV of the present work might be attributed to the limited energy

resolution of inverse photoemission and uncertainties of the Fermi level pinning, which was taken from the literature in Ref. 11. Reflectance-anisotropy spectroscopy also finds a spectral feature at 3 eV on the  $c(4 \times 2)$  surface, which is assigned to a transition between surface states.<sup>25</sup> This agrees well with the resonance between the occupied surface state  $D_{up}$  and the dimer-bond state at 2.83 eV. Optical techniques are, however, not able to pinpoint the location of the transitions in momentum space.

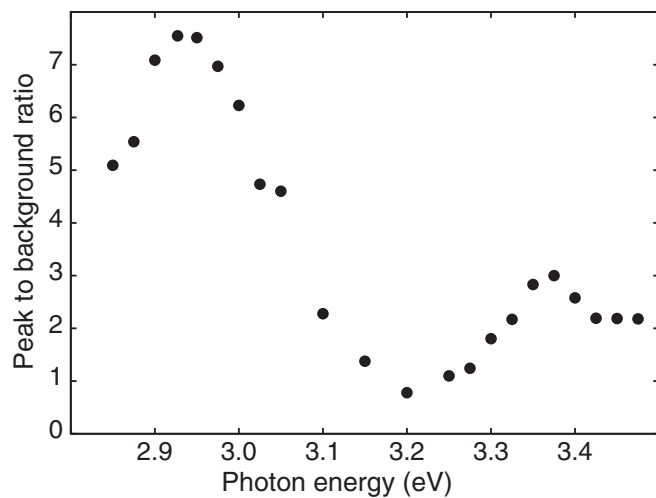


FIG. 6. Intensity of the  $D_{up}$  surface state normalized to the intensity at the low-energy background as a function of photon energy.

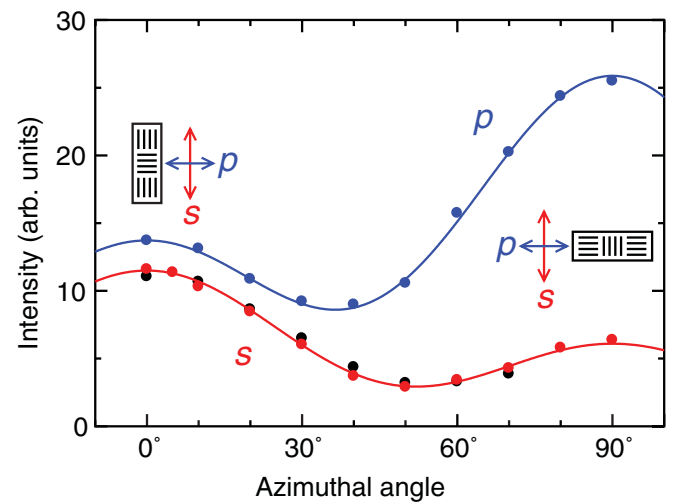


FIG. 7. (Color online) Azimuthal dependence of the dimer-bond resonance for  $s$ - and  $p$ -polarized light for a photon energy of 2.97 eV.



The occupied dangling-bond state  $D_{\text{up}}$  shows a downward dispersion described by a negative effective mass of  $0.50 \pm 0.05$  in units of the free-electron mass. This value is also found near the resonant transition via the dimer-bond state (see Fig. 3). A similar behavior has been observed for resonant transitions via an image-potential state.<sup>26</sup> The positive dispersion of the image-potential state is observed only for photon energies above resonance. For higher photon energies, the dimer-bond state is observed only as a weak broad peak and a reliable dispersion could not be determined. The negative dispersion of the  $D_{\text{up}}$  state is found in most experimental one- and two-photon photoemission studies over a wide range of photon energies.<sup>4,8,17,26</sup> However, most band-structure calculations find a positive dispersion.<sup>7,17,27</sup> Slab calculations are faced with the difficulty of identifying the surface state among the manifold of bands derived from the downward-dispersing bulk bands near the valence-band maximum. Nevertheless, calculations find an upward dispersion in contrast to experimental observations. In order to clarify this discrepancy, it would be worthwhile to investigate the photoemission spectral function of a discrete surface state on a background of bulk bands in more detail. Recent progress toward a nonperturbative approach to photoemission by direct simulation of photocurrents has been reported.<sup>28</sup> For two-photon photoemission, a two-state double-continuum Fano resonance has been considered recently.<sup>23</sup>

## V. SUMMARY

Two-photon photoemission was used to identify the unoccupied dimer-bond state on the Si(001) surface 2.83 eV above the valence-band maximum. A strong resonance enhancement

for photon energies around 3 eV is found for excitation from the occupied dangling-bond state  $D_{\text{up}}$ . The azimuthal dependence observed on samples with unequal percentages of the two domains ( $1 \times 2$ ) and ( $2 \times 1$ ) proves the orientation of the observed state along the dimer axis. This approach to identify the orientation of orbitals might be applied to many other systems. The polarization behavior is also in agreement with an orbital of even symmetry aligned along the dimer axis. Previous two-photon- and inverse-photoemission experiments reported results that can seamlessly be reconciled with the unoccupied dimer-bond state. The dispersion at resonance is dominated by the occupied initial state  $D_{\text{up}}$ . Its downward dispersion is described by  $-0.50$  free-electron masses and has been observed in many one- or two-photon photoemission experiments, in contrast to results from band-structure calculations.

The dimer-bond state is located in the continuum of the conduction band with a resulting large linewidth of 0.14 eV. This would correspond to a lifetime around 5 fs at the limit of current experimental capabilities. However, the measured linewidth might also contain contributions from defects<sup>29</sup> or vibrational excitations. The minimum at energies above the resonance in Fig. 6 is similar to the Fano-type effects seen for the image-potential resonance on Si(001) excited from the occupied dangling-bond state  $D_{\text{up}}$ .<sup>23</sup> Scanning tunneling microscopy should also be able to image the dimer bond at the reported energy. The relevance of the resonant excitation into the antibonding dimer bond for laser-stimulated processes or desorption would be of considerable interest for further studies. Indeed, a strong increase of the laser-induced desorption rate is observed for photon energies around 3 eV on Si(001),<sup>13</sup> but not on Si(111).<sup>30</sup>

- 
- <sup>1</sup>H. Okada, Y. Fujimoto, K. Endo, K. Hirose, and Y. Mori, *Phys. Rev. B* **63**, 195324 (2001).
- <sup>2</sup>F. J. Himpsel and D. E. Eastman, *J. Vac. Sci. Technol.* **16**, 1297 (1979).
- <sup>3</sup>R. I. G. Uhrberg, G. V. Hansson, J. M. Nicholls, and S. A. Flodström, *Phys. Rev. B* **24**, 4684 (1981).
- <sup>4</sup>Y. Enta, S. Suzuki, and S. Kono, *Phys. Rev. Lett.* **65**, 2704 (1990).
- <sup>5</sup>M. Rohlfing, P. Krüger, and J. Pollmann, *Phys. Rev. B* **52**, 13753 (1995).
- <sup>6</sup>Z. Zhu, N. Shima, and M. Tsukada, *Phys. Rev. B* **40**, 11868 (1989).
- <sup>7</sup>A. Ramstad, G. Brocks, and P. J. Kelly, *Phys. Rev. B* **51**, 14504 (1995).
- <sup>8</sup>G. V. Hansson and R. I. G. Uhrberg, *Surf. Sci. Rep.* **9**, 197 (1988).
- <sup>9</sup>L. S. O. Johansson, R. I. G. Uhrberg, P. Martensson, and G. V. Hansson, *Phys. Rev. B* **42**, 1305 (1990).
- <sup>10</sup>L. S. O. Johansson and B. Reihl, *Surf. Sci.* **269-270**, 810 (1992).
- <sup>11</sup>J. E. Ortega and F. J. Himpsel, *Phys. Rev. B* **47**, 2130 (1993).
- <sup>12</sup>J. Xu, S. H. Overbury, and J. F. Wendelken, *Phys. Rev. B* **53**, 4245 (1996).
- <sup>13</sup>J. Kanasaki, M. Nakamura, K. Ishikawa, and K. Tanimura, *Phys. Rev. Lett.* **89**, 257601 (2002).
- <sup>14</sup>C. Kentsch, M. Kutschera, M. Weinelt, Th. Fauster, and M. Rohlfing, *Phys. Rev. B* **65**, 035323 (2001).
- <sup>15</sup>K.-I. Shudo and T. Munakata, *Phys. Rev. B* **63**, 125324 (2001).
- <sup>16</sup>T. Ichibayashi, S. Tanaka, J. Kanasaki, K. Tanimura, and Th. Fauster, *Phys. Rev. B* (to be published).
- <sup>17</sup>M. Weinelt, M. Kutschera, Th. Fauster, and M. Rohlfing, *Phys. Rev. Lett.* **92**, 126801 (2004).
- <sup>18</sup>P. Krüger and J. Pollmann, *Phys. Rev. B* **38**, 10578 (1988).
- <sup>19</sup>J. Pollmann, R. Kalla, P. Krüger, A. Mazur, and G. Wolfgarten, *Appl. Phys. A* **41**, 21 (1986).
- <sup>20</sup>J. Pollmann, A. Mazur, and M. Schmeits, *Physica B* **117-118**, 771 (1983).
- <sup>21</sup>M. Rohlfing, P. Krüger, and J. Pollmann, *Phys. Rev. B* **48**, 17791 (1993).
- <sup>22</sup>M. Rohlfing, P. Krüger, and J. Pollmann, *Phys. Rev. B* **52**, 1905 (1995).
- <sup>23</sup>C. Eickhoff, M. Teichmann, and M. Weinelt, *Phys. Rev. Lett.* **107**, 176804 (2011).
- <sup>24</sup>F. J. Himpsel and Th. Fauster, *J. Vac. Sci. Technol. A* **2**, 815 (1984).
- <sup>25</sup>M. Palumbo, N. Witkowski, O. Pluchery, R. Del Sole, and Y. Borenstein, *Phys. Rev. B* **79**, 035327 (2009).
- <sup>26</sup>M. Kutschera, M. Weinelt, M. Rohlfing, and Th. Fauster, *Appl. Phys. A* **88**, 519 (2007).
- <sup>27</sup>J. E. Northrup, *Phys. Rev. B* **47**, 10032 (1993).
- <sup>28</sup>H. Husser, J. van Heys, and E. Pehlke, *Phys. Rev. B* **84**, 235135 (2011).
- <sup>29</sup>K. Boger, Th. Fauster, and M. Weinelt, *New J. Phys.* **7**, 110 (2005).
- <sup>30</sup>K. Tanimura and J. Kanasaki, *J. Phys. Condens. Matter* **18**, S1479 (2006).